Absolute differential cross sections for small-angle He^+-He elastic and charge-transfer scattering at keV energies

R. S. Gao, L. K. Johnson, D. A. Schafer, J. H. Newman, K. A. Smith, and R. F. Stebbings
Department of Physics, Department of Space Physics and Astronomy, and Rice Quantum Institute, Rice University, P.O. Box 1892, Houston, Texas 77251
(Received 7 March 1988)

This paper reports measurements of absolute differential cross sections for elastic and for charge-transfer scattering in He^+-He collisions. Elastic-scattering cross sections have been determined at 1.5 keV over the laboratory angular range 0.04°–1.0° while charge-transfer cross sections have been determined at 1.5, 2.5, and 5.0 keV over the range 0.02°–1.0°, and at 0.25 and 0.50 keV over the range 0.02°–7.8°. The experimental data exhibit strong oscillations over the range of angles and energies studied and are in agreement with partial-wave theory calculations using phase shifts derived from proposed forms of the *gerade* and *ungerade* He_2^+ interaction potentials. The experimental cross sections have also been integrated over angle to provide absolute integral cross sections.

I. INTRODUCTION

Numerous studies of differential scattering in ion-neutral collisions have been reported in the literature. Notable among these in the context of the present work is that of Lorents and Aberth,[1] who measured differential cross sections for the elastic scattering of He^+ ions by He in the 20–600 eV energy range. Important contributions were also made by Ziemba *et al.*,[2] Everhart,[3] Lockwood *et al.*,[4] Baudon *et al.*,[5] Dhuicq *et al.*,[6] Barat *et al.*,[7] Brenot *et al.*,[8] Bordenave-Montesquieu and Dagnac,[9] Fleischmann *et al.*,[10] Nagy *et al.*,[11] Eriksen *et al.*,[12] and Pol *et al.*[13] There is, however, surprisingly little published information on absolute cross sections for differential scattering. This paper reports experimental absolute cross sections for charge transfer and elastic scattering of ground-state, keV-energy helium ions from neutral helium. The high angular resolution of the apparatus allows detailed observations of symmetry oscillations in the vicinity of the classical rainbow maximum. The experimental data are in excellent agreement with theoretical cross sections calculated from the He_2^+ interaction potentials proposed by Marchi and Smith.[14] Such comparisons provide a test of the molecular potentials at internuclear distances of a few angstroms. Total cross sections, determined by integrating the differential cross sections over angle, are in good agreement with those measured previously by other investigators.

II. APPARATUS AND EXPERIMENTAL METHOD

Figure 1 shows a schematic of the apparatus, which has been described in detail in previous publications.[15] Helium ions emerging from the electron-impact ion source are accelerated to the desired energy and focused by an electrostatic lens. The resulting beam is momentum analyzed by a pair of 60° sector magnets and passes through a collimating aperture before arriving at the target cell (TC). A position-sensitive detector (PSD) is located on axis downstream to monitor both the primary ion beam and fast collision products. Deflection plates (DP's) can be used to prevent primary and scattered ions from striking the detector. An LSI 11/2 microcomputer monitors the output of the PSD electronics, sorting the arrival coordinates of each detected particle into a square 90-bin × 90-bin array. The physical area corresponding to the bin size is chosen to meet the resolution requirements of the experiment. The minimum physical bin size for the present experiments is $109 \times 109\ \mu m^2$. Measurement of this bin size is accomplished by observing the shadow of a nickel grid of known dimensions placed directly in front of the detector as an ion beam is swept over the detector surface. This technique is also used to measure the position-determining accuracy of the PSD.

Two different configurations of the apparatus are employed; one to collect data from very-small-angle scattering (0.01°–1.0°), and another for larger-angle scattering (1.0°–7.8°). In the very-small-angle configuration, the collimating aperture and the entrance aperture of the target cell are 20 and 30 μm in diameter, respectively, and are separated by 49 cm, collimating the ion beam to less than 0.003° divergence. The TC has a length of 0.35 cm and an exit aperture 300 μm in diameter. A PSD with an

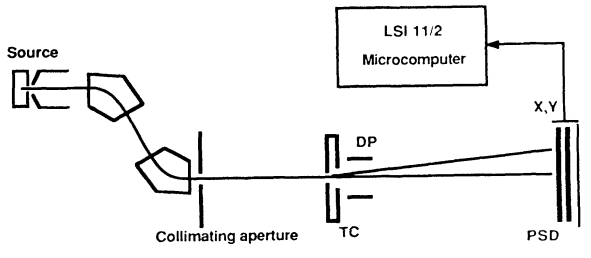

FIG. 1. Schematic of the apparatus.

active area 4.0 cm in diameter is axially located 109 cm beyond the TC, limiting the maximum observable scattering angle to about 1.3°. In the larger-angle configuration, the aperture diameters are unchanged, but the distance between the collimating aperture and the TC is shortened to 10 cm, while the length of the TC itself is reduced to 0.03 cm. A 2.5-cm-diam PSD located 11 cm beyond the TC is positioned slightly off axis so that the scattering pattern is displaced by the PSD center, allowing a maximum observed scattering angle of 8.4°.

Under the thin target conditions used in this experiment, the differential cross section is related to the measured quantities by the expression

$$\frac{d\sigma(\theta)}{d\Omega}=\frac{\Delta S(\theta)}{SnL\Delta\Omega}\ , \tag{1}$$

where S is the primary ion beam flux in particles per second, $\Delta S(\theta)$ is the neutral flux scattered at laboratory angle θ into a solid angle $\Delta\Omega$ steradians, n is the target number density (obtained from a measurement of the TC gas pressure), and L is the physical length of the cell. At a typical TC pressure of 5 mtorr, the residual vacuum chamber pressure is maintained below 2×10^{-7} torr. Under these conditions, only 5% of the beam is scattered by the target gas, making multiple collision effects negligible.

A detailed description of the data acquisition and analysis technique has been given by Nitz *et al.*[15] and only a brief discussion will be provided here. Two data sets are taken, one with gas in the target cell and one without. The scattered flux $\Delta S(\theta)$ is obtained by organizing the 90×90 data arrays into concentric rings and subtracting the gas-out data from the gas-in data. This procedure also discriminates between counts due to scattering from the target gas and counts arising from other sources, such as PSD dark counts or scattering from the background gas or from edges of apertures.

During charge-transfer measurements the ions emerging from the TC are electrostatically deflected away from the PSD so that only the neutral collision products are detected. During measurements of elastic scattering, however, the now unwanted neutral products of charge transfer inevitably strike the detector, and the gas-in data therefore include counts due to the primary beam and to both charged and neutral collision products. An additional data set is therefore taken with plates DP activated to remove charged particles from the beam and is subtracted from the gas-in data set, providing an array containing only counts resulting from charged-particle impacts. It is from this array that the gas-out data array is then subtracted to obtain the elastic-scattering signal.

The procedures for measuring the primary beam flux for elastic-scattering and charge-transfer cross sections differ slightly. During measurements of elastic scattering the primary beam continuously strikes the detector, while for studies of charge transfer, the primary beam is deflected away. Therefore, at regular intervals during the charge-transfer data accumulation, the deflection plates are turned off and the primary beam flux is recorded.

The experimental uncertainty in the number of counts at a particular angle is primarily statistical, and ranges from 1% near 0.02° to 10% near 8°. The angular uncertainty arises from the finite width of the primary ion beam, the discrete width of the analysis rings, and electronic errors in the detector's position-encoding circuits, and amounts to about 0.02° at the smallest scattering angles. The effect of the finite angular resolution of the apparatus has been estimated by calculating the convolution of the theoretical cross sections with an apparatus function that accounts for the above-mentioned effects.

III. THEORETICAL CONSIDERATIONS

The calculations take account of the fact that for He^+-He collisions the electronic Hamiltonian is symmetric. Two electronic states therefore result when a ground-state helium atom and ion are brought together adiabatically, one of which is symmetric (g) and the other antisymmetric (u). Scattering occurs from each of these potentials with amplitudes $f_g(\phi)$ and $f_u(\phi)$, where ϕ denotes the center-of-mass scattering angle. Since the nuclei are indistinguishable it is impossible to determine whether a particle detected at a given angle in the laboratory frame is a scattered projectile atom or "knocked-on" recoil target atom. In consequence, the additional amplitudes $f_{g,u}(\pi-\phi)$ must be included and the differential cross sections are given by[14]

$$\left.\frac{d\sigma(\phi)}{d\Omega}\right|_{\text{(elastic)}}=\tfrac{1}{4}\,|\,f_g(\phi)+f_u(\phi)+f_g(\pi-\phi)-f_u(\pi-\phi)\,|^2\ , \tag{2}$$

$$\left.\frac{d\sigma(\phi)}{d\Omega}\right|_{\text{(transfer)}}=\tfrac{1}{4}\,|\,f_g(\phi)-f_u(\phi)+f_g(\pi-\phi)+f_u(\pi-\phi)\,|^2\ . \tag{3}$$

For angles less than 1° however, the $f_{g,u}(\pi-\phi)$ are negligible compared with the $f_{g,u}(\phi)$, and the cross sections are well represented by the expressions

$$\left.\frac{d\sigma(\phi)}{d\Omega}\right|_{\text{(elastic)}}=\tfrac{1}{4}\,|\,f_g(\phi)+f_u(\phi)\,|^2\ , \tag{4}$$

$$\left.\frac{d\sigma(\phi)}{d\Omega}\right|_{\text{(transfer)}}=\tfrac{1}{4}\,|\,f_g(\phi)-f_u(\phi)\,|^2\ . \tag{5}$$

The scattering amplitudes are given by

$$f_{g,u}(\phi)=\frac{1}{2ik}\sum_{l=0}^{\infty}(2l+1)(e^{2i\delta_l^{g,u}}-1)P_l(\cos\phi)\ , \tag{6}$$

where k is the wave number and $\delta_l^{g,u}$ is the phase shift of the lth partial wave. A semiclassical JWKB approximation is used to determine the phase shifts from the potentials of Marchi and Smith[14] (as discussed in Nitz *et al.*[15]), and the phase shifts are directly summed via Eq. (6). Typically a few thousand phase shifts are used. The scattering amplitudes are then combined as shown above to obtain differential cross sections, which are transformed into laboratory coordinates for comparison to experimental results. The calculated cross sections exhibit detailed structure, the most pronounced of which is

a periodic undulation as a function of scattering angle, which arises[1,7,14] as the result of interference between the different scattering amplitudes.

IV. RESULTS AND DISCUSSION

In order to derive absolute experimental cross sections, the detector efficiency for scattered particles must be known relative to the efficiency for the primary beam particles. In the case of elastic scattering the primary beam and the scattered particles are identical. They are therefore detected with equal efficiency and absolute cross sections are thus derived from the experimental signal without ambiguity. However, in placing the charge-transfer data on an absolute footing a difficulty arises because the primary and product particles are now different and their detection efficiencies are no longer necessarily the same. Nagy *et al.*[11] addressed this problem and offered an ingenious solution. They noted that while both the elastic-scattering and charge-transfer cross sections individually exhibit oscillatory behavior due to the interference between the scattering amplitudes, their sum is free from such oscillations (the interference terms cancel) and decreases monotonically with increasing angle. It follows that if the detection efficiencies of the ions and the neutral atoms are different, the combined *signals* from elastic scattering and charge transfer will exhibit this oscillatory structure with a phase and amplitude that is determined by the particular values of these efficiencies. No such oscillatory behavior is, however, discernible in the combined data, and the detection efficiencies of helium atoms and ions are thus identical to within experimental uncertainty. This result is consistent with other direct measurements made in this laboratory[15] of PSD detection efficiencies for keV ions and atoms, and so experimental cross sections have been determined on this basis.

Raw data for both elastic and charge-transfer scattering are shown in Fig. 2, which depicts the contents of the 90×90 array. The vertical displacement indicates the number of counts at a given location on the detector, while the horizontal axes correspond to the plane of the detector surface. In Fig. 3 are shown experimental and

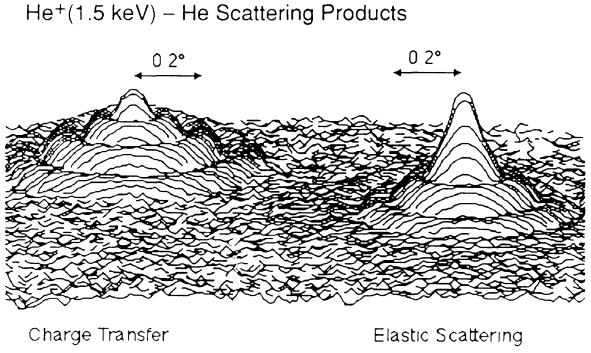

FIG. 2. Distribution of counts on the detector for 1.5 keV charge-transfer scattering.

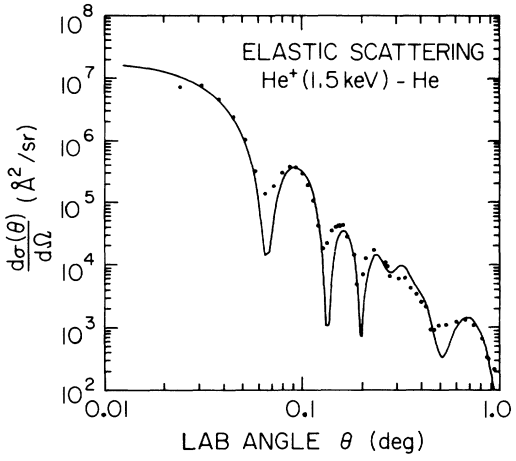

FIG. 3. Experimental points and theoretical prediction for differential cross sections for elastic scattering at a projectile energy of 1.5 keV.

calculated elastic-scattering cross sections at 1.5 keV projectile energy. Cross sections for charge transfer at 0.25, 0.50, 1.5, 2.5, and 5.0 keV projectile energies are shown in Figs. 4 and 5 together with theoretical results.

The agreement between experiment and theory is good, with the calculations showing rather more pronounced oscillations than do the experiments. The convolution of the theoretical results with the apparatus effects brings the theory and experiment into better agreement, as shown in Fig. 6. It should be noted that the calculations

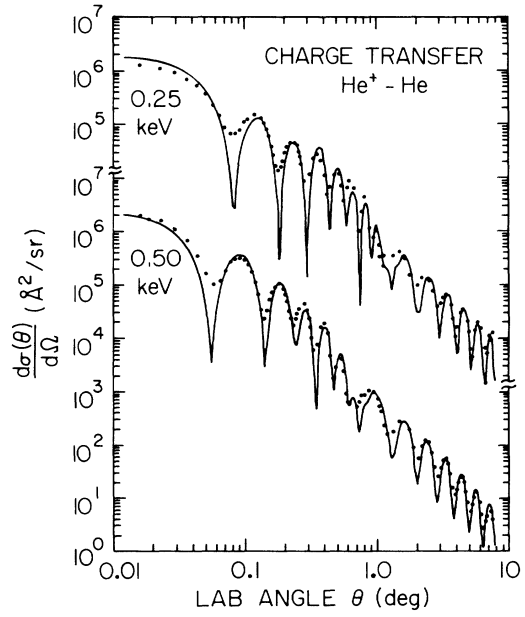

FIG. 4. Experimental points and theoretical prediction for differential cross sections for charge-transfer scattering at projectile energies of 0.25 and 0.50 keV.

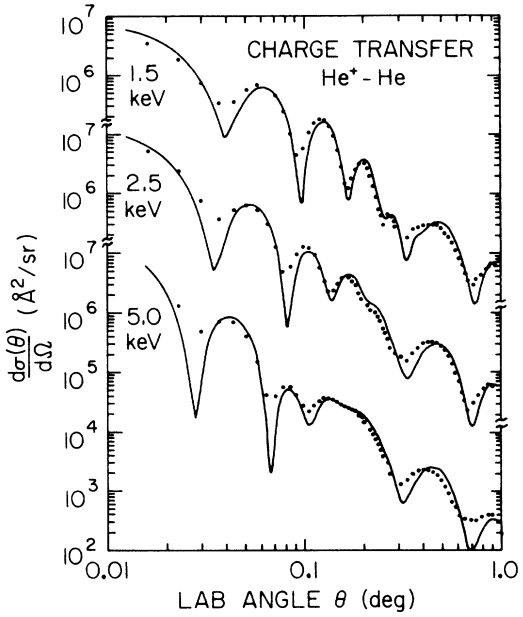

FIG. 5. Experimental points and theoretical prediction for differential cross sections for charge-transfer scattering at projectile energies of 1.5, 2.5, and 5.0 keV.

include no adjustable parameters. Figure 4, containing 0.25 and 0.50 keV charge-transfer data, is of particular interest since these measurements span the largest range of scattering angles. At angles above about 1°, the angular positions of the maxima and minima in the cross sections are seen to be independent of projectile energy—a result that has been discussed by Lorents and Aberth,[1] Lockwood *et al.*,[4] and Eriksen *et al.*[12] However, below about 1° the oscillations are less regular and their angular

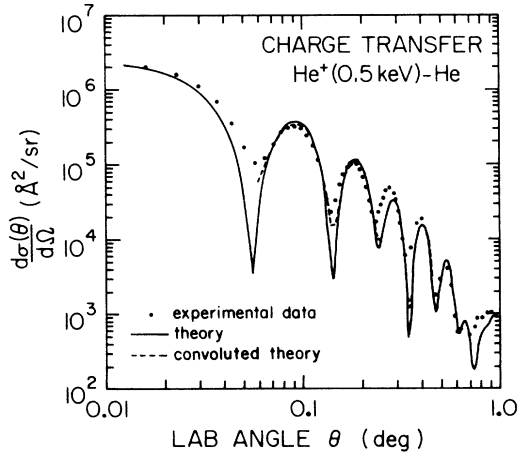

FIG. 6. Experimental points and theoretical prediction for differential cross sections for charge-transfer scattering at a projectile energy of 1.5 keV, including the prediction of a convolution of the theory with a function characteristic of the angular resolution of the apparatus.

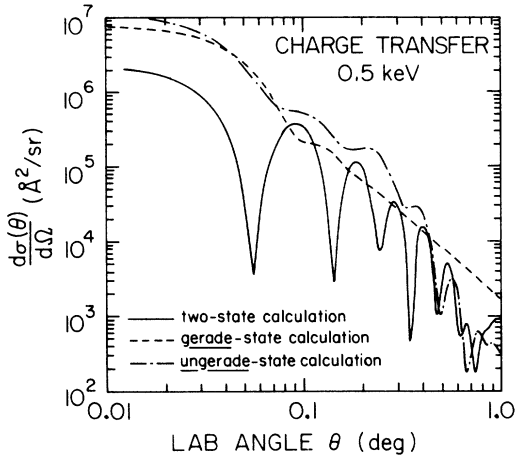

FIG. 7. Theoretical calculations for single-potential scattering from the lowest-lying *gerade* and *ungerade* potentials of He_2^+ for a projectile energy of 0.5 keV.

positions are no longer energy independent; instead, a complex structure in this region arises as a consequence of three independent effects. First, the interference between the gerade and ungerade scattering amplitudes is still responsible for large oscillations in the cross sections. Second, classical trajectory-dependent effects, such as "rainbow" scattering from the attractive ungerade potential, become important. This has been confirmed through calculations of the classical deflection function for the *ungerade* potential, and the effect of the attractive well is also apparent in the calculations shown in Fig. 7, which show differential cross sections calculated for the *ungerade* and *gerade* potentials individually. Third, diffraction of the matter wave of the projectile by the tar-

TABLE I. Integrated absolute differential cross sections for He^+-He processes. ES represents elastic scattering and CT charge transfer.

Energy (keV)	Integrated σ (Å^2) (angular range)	Other investigators
0.25 (CT)	13 (0.002°–7.0°)	13[a,b]
0.5 (CT)	12 (0.002°–7.0°)	12[a,b]
1.5 (ES)	7.2 (0.04°–1.0°)	
1.5 (CT)	7.6 (0.002°–1.0°)	10[c], 9.9[d]
2.5 (CT)	6.9 (0.002°–1.0°)	8.9[c,d]
5.0 (CT)	5.8 (0.002°–1.0°)	7.7[c], 7.6[d]

[a]Reference 16.
[b]Reference 17.
[c]Reference 18.
[d]Reference 19.

get potential causes gentle small-angle undulations in the cross sections. These undulations are consistently present in both experimental and calculated differential cross sections for neutral-neutral scattering,[15] and take their character from the repulsive wall of the interatomic potential. Such undulations are apparent in the cross section calculated from the *gerade* potential in Fig. 7.

The measured differential cross sections have been integrated over the observed angular range. Table I gives these integrated cross sections along with total cross sections determined by Rundel *et al.*,[16] Hodgkinson and Briggs,[17] Eisele and Nagy,[18] and Hegerberg *et al.*[19] The values compare particularly favorably for the 0.25 and 0.50 keV data, where the angular range spanned by the data is the largest.

V. SUMMARY

The angular distributions of energetic charged and neutral products of He^+-He collisions have been measured. Both distributions are governed by the same pair of He_2^+ potentials; the charge state of the detected particle resulting from a given collision is simply dependent upon which of the two nuclei the active electron ultimately resides in. Given the form of the He_2^+ potentials the scattering amplitudes $f_{g,u}(\phi,\pi-\phi)$ have been calculated and then combined appropriately to yield cross sections for charge transfer and elastic scattering. Experiment and theory agree very well for both processes, giving a high degree of confidence in the He_2^+ potentials. These results furthermore demonstrate a new capability to measure high-resolution, small-angle, absolute differential cross sections for positive ions at keV energies. The technique may be extended to other targets and projectiles, both atomic and molecular, and several experiments are underway in this laboratory.

ACKNOWLEDGMENTS

The authors thank D. E. Nitz for his computer codes, N. F. Lane and M. Kumura for productive discussions, and P. S. Gibner for assistance in the initial data taking. This work has been supported by the Robert A. Welch Foundation, National Aeronautics and Space Administration, and the National Science Foundation Atmospheric Sciences Section.

[1]D. C. Lorents and W. Aberth, Phys. Rev. **139**, A1017 (1965).
[2]F. P. Ziemba, G. J. Lockwood, G. H. Morgan, and E. Everhart, Phys. Rev. **118**, 1552 (1960).
[3]E. Everhart, Phys. Rev. **132**, 2083 (1963).
[4]G. J. Lockwood, H. F. Helbig, and E. Everhart, Phys. Rev. **132**, 2078 (1963).
[5]J. Baudon, M. Barat, and M. Abignoli, J. Phys. B **1**, 1083 (1968).
[6]D. Dhuicq, J. Baudon, and M. Barat, J. Phys. B **6**, L1 (1973).
[7]M. Barat, J. C. Brenot, and J. Pommier, J. Phys. B **6**, L105 (1973).
[8]J. C. Brenot, J. Pommier, D. Dhuicq, and M. Barat, J. Phys. B **8**, 448 (1975).
[9]D. Bordenave-Montesquieu and R. Dagnac, J. Phys. B **12**, 1233 (1979).
[10]H. H. Fleischmann, R. A. Young, and J. W. McGowan, Phys. Rev. **153**, 19 (1967).
[11]S. W. Nagy, S. M. Fernandez, and E. Pollack, Phys. Rev. A **3**, 280 (1971).
[12]F. J. Eriksen, S. M. Fernandez, and E. Pollack, Phys. Rev. A **5**, 2443 (1972).
[13]V. Pol, W. Kauppila, and J. T. Park, Phys. Rev. A **8**, 2990 (1973).
[14]R. P. Marchi and F. T. Smith, Phys. Rev. **139**, A1025 (1965); see also W. L. Lichten, *ibid.* **131**, 229 (1963); P. N. Reagan, J. C. Browne, and F. A. Matsen, *ibid.* **132**, 304 (1963); P. E. Phillipson, *ibid.* **125**, 1981 (1962); H. S. W. Massey and R. A. Smith, Proc. R. Soc. London, Ser. A **142**, 142 (1933).
[15]D. E. Nitz, R. S. Gao, L. K. Johnson, K. A. Smith, and R. F. Stebbings, Phys. Rev. A **35**, 4541 (1987); R. S. Gao, P. S. Gibner, J. H. Newman, K. A. Smith, and R. F. Stebbings, Rev. Sci. Instrum. **55**, 1756 (1984); R. S. Gao, L. K. Johnson, D. E. Nitz, K. A. Smtih, and R. F. Stebbings, Phys. Rev. A **36**, 3077 (1987).
[16]R. D. Rundel, D. E. Nitz, K. A. Smith, M. W. Geis, and R. F. Stebbings, Phys. Rev. A **19**, 33 (1979).
[17]D. P. Hodgkinson and J. S. Briggs, J. Phys. B **9**, 255 (1976).
[18]F. L. Eisele and S. W. Nagy, J. Chem. Phys. **65**, 752 (1976).
[19]R. Hegerberg, T. Stefánsson, and M. T. Elford, J. Phys. B **11**, 133 (1978).